The electromagnetic properties of nanoparticle colloids at radio and microwave frequencies



2007 J. Phys. D: Appl. Phys. 40 5331

(http://iopscience.iop.org/0022-3727/40/17/048)

IOP Publishing Journal of Physics D: Applied Physics
J. Phys. D: Appl. Phys. **40** (2007) 5331–5337 doi:10.1088/0022-3727/40/17/048

# The electromagnetic properties of nanoparticle colloids at radio and microwave frequencies

**Shahid Hussain**[1], **Ian J Youngs**[2] **and Ian J Ford**[3]

[1] Energy and Materials Department, QinetiQ Limited, Cody Technology Park, Farnborough, Hampshire, GU14 0LX, UK
[2] Physical Sciences Department, DSTL, Porton Down, Salisbury, Wiltshire, SP4 0JQ, UK
[3] Department of Physics and Astronomy, University College London, Gower Street, London, WC1E 6BT, UK

Received 29 May 2007
Published 16 August 2007
Online at stacks.iop.org/JPhysD/40/5331

**Abstract**
The aim of this study is to investigate the electromagnetic properties of nanoparticle colloids in the frequency range 1 MHz–20 GHz, with focus on the electromagnetic absorption mechanisms at microwave frequencies. A broad range of magnetic and dielectric properties are investigated and a number of mechanisms are highlighted for tailoring the electromagnetic performance. Results from the $Co_xNi_{1-x}$ series, with particle sizes ranging from 25 to 200 nm, show particle size-related dielectric and magnetic properties, which aid the optimization of the resulting properties, in addition to conventional mechanisms, which are also demonstrated in colloidal form. A further reduction in particle size to below 20 nm leads to single magnetic domain particles, which also exhibit enhanced electromagnetic properties, as demonstrated with broadband magnetic performance achieved for Co ferrofluid with an average particle size of 5 nm.

## 1. Introduction

Electromagnetic applications rely on the interaction of materials with electromagnetic fields. The design of effective electromagnetic materials therefore requires control over the electric and magnetic components within these materials, which can then interact with the time-varying electric and magnetic field components associated with the electromagnetic fields. This paper summarizes research into the electromagnetic properties of nanoparticle colloids at radio and microwave frequencies ranging from 1 MHz to 20 GHz. The motivation of the work stems from the need to explore systems exhibiting losses at microwave frequencies, enabling electromagnetic control and screening applications.

Enhancement of the electromagnetic properties requires enhanced dielectric and magnetic properties, such as loss mechanisms associated with conduction or resonance and relaxation phenomena. Conventional electromagnetic applications have mainly relied on micron-scale particle sizes. With advances in nanotechnology, electromagnetic materials have steadily moved towards smaller size regimes. As the particle size decreases to the nanoscale, changes in the electromagnetic properties can be expected and even enhanced, with the emerging possibility of additional loss mechanisms and faster charge dynamics [1, 2].

Nanoparticle colloids can be incorporated into a range of structures because of their small particle sizes, without significantly affecting mechanical properties such as weight and flexibility. Nanoparticle colloids, with tailored electromagnetic properties, could potentially be used in a number of applications, such as radar absorbing materials, electromagnetic shielding, tissue imaging [3] and inks for magnetic recording technology [4].

Section 2 discusses the fundamental electromagnetic properties of nanoparticle colloids. The nanoparticle and colloidal combinations investigated are described in the experimental details in section 3. The results are summarized in section 4 and the conclusions arising from the study are discussed in section 5.

## 2. Electromagnetic properties of nanoparticle colloids

The fundamental electromagnetic properties have been extensively reported elsewhere [1, 5] and so will only briefly be summarized in this section.

The dielectric properties of the colloids are discussed here in terms of the complex dielectric constant or effective permittivity:

$$\varepsilon(\omega) = \varepsilon'(\omega) - \mathrm{i} \cdot \varepsilon''(\omega), \tag{1}$$

where $\varepsilon'$ and $\varepsilon''$ are the real and imaginary components of permittivity, $\varepsilon$, respectively. The term $\varepsilon'$ is associated with energy storage and $\varepsilon''$ is associated with loss or energy dissipation within a material. Dielectric loss can result from electrical conduction processes and mechanisms of both dielectric resonance [5] (a periodic process associated with regular oscillations of any part of a system, such as the response of individual atoms or molecules) and relaxation [5] (associated with the response of electric dipoles, such as dipolar relaxation in water [6]).

The magnetic properties of the colloids are described by the complex permeability:

$$\mu(\omega) = \mu' - \mathrm{i} \cdot \mu''(\omega) \tag{2}$$

where $\mu'$ is the real (energy storage) part and $\mu''$ is the imaginary (loss) part of the permeability.

Optimization of the permittivity and permeability can be of great benefit in a number of electromagnetic absorption applications [3, 5], such as EMC (electromagnetic compatibility) in buildings to absorb stray mobile phone signals. The electromagnetic requirements for microwave absorption are well-established [7]. The first requirement is to maximize the electromagnetic radiation entering the structure, by minimizing front-face reflection. This is ideally achieved if the real and imaginary components of the complex permittivity, $\varepsilon$, and permeability, $\mu$, are separately equal, which results in perfect impedance match between the material and free space. The second requirement is that the signal is sufficiently attenuated once the radiation has entered the material, which is met for high values of imaginary permittivity and permeability.

The main magnetic loss mechanisms at microwave frequencies result from ferromagnetic resonance [8] and superparamagnetism [9].

Ferromagnetic resonance occurs due to the precessional motion of the magnetic dipole moments [8]. This is a periodic process, which absorbs energy from the applied field at a specific frequency, known as ferromagnetic resonance or Larmor frequency, $f_{\mathrm{L}}$:

$$f_{\mathrm{L}} = \frac{\mu_0 \gamma_{\mathrm{m}} H_{\mathrm{A}}}{2\pi}, \tag{3}$$

where $H_{\mathrm{A}}$ represents the anisotropy field associated with the direction of the magnetic moment with respect to the crystallographic axes, $\mu_0$ is the free space permeability and $\gamma_{\mathrm{m}}$ is the gyromagnetic ratio.

Superparamagnetism is a property of particles so small (<20 nm) that only single magnetic domains can exist within them. The magnetic moment can have parallel and antiparallel equilibrium orientations along an axis through the particle. The magnetic moment will lie along these directions separated by an anisotropy energy barrier of $E = K V_{\mathrm{p}}$ (where $K$ is the anisotropy constant [8] and $V_{\mathrm{p}}$ is the particle volume). The small particle size associated with superparamagnetic particles results in a smaller energy barrier, which leads to a relaxation loss mechanism (known as Néel relaxation), associated with the spontaneous changes in the direction of magnetization [10]. The process results in energy absorption from the applied field.

## 3. Experimental details

Measurements of the electromagnetic properties of the colloids were carried out using two different experimental techniques in order to cover a broad frequency range:

- The high frequency measurements (500 MHz–18 GHz) were carried out using the HP 8510C Vector Network Analyser (VNA), with a synthesized frequency sweeper. The VNA measured the complex scattering, $S$, parameters [7] associated with transmission and reflection from the test samples, from which the permeability, $\mu$, and permittivity, $\varepsilon$, were obtained using the Nicholson and Ross method [7].
- The low frequency measurements (1.0 MHz–1.8 GHz) were carried out using the broadband Novocontrol Spectrometer [11] with a HP 4291 Vector Network Analyser, using a coaxial line reflection technique, from which the permeability and permittivity were determined.

### 3.1. $Co_xNi_{1-x}$ Nanoparticles

A range of $\mathrm{Co}_x\mathrm{Ni}_{1-x}$ particles were synthesized within the Energy & Materials Centre at QinetiQ. The $\mathrm{Co}_x\mathrm{Ni}_{1-x}$ samples consisted of five concentrations of cobalt to nickel, with $x = 0$ (Ni only), 0.2, 0.5, 0.8 and 1 (Co only). These ranged from particle sizes of 25–200 nm to ensure that potential particle size-related effects could be investigated thoroughly.

Each of the particle combinations was dispersed in paraffin wax at volume fractions ranging from 0.05 to 0.40 (particles to wax). This was achieved by firstly stirring the $\mathrm{Co}_x\mathrm{Ni}_{1-x}$ powder samples in hexane to reduce agglomeration of the magnetic nanoparticles and ensure homogeneous samples. The nanoparticles were then dispersed in molten wax and stirred until cooling led to solidification. A press was used to make coaxial test samples (outer diameter = 6.995mm, inner diameter = 3.045 mm) by applying a constant pressure of 0.8 ton for 30 s to each of the samples. The electromagnetic properties of the samples were then measured in the frequency range 0.5–18.0 GHz using the HP 8510C VNA system.

### 3.2. Magnetite nanoparticles

Magnetite ($\mathrm{Fe_3O_4}$) nanoparticles were synthesized within the Energy & Materials Centre at QinetiQ. The samples were composed of particles with an average diameter of 8 nm and were dispersed in a solid matrix of stearic acid at a volume fraction of 0.22. The small particle sizes were selected to ensure single domain particles. In addition to high frequency (0.5–18.0 GHz) measurements using the HP 8510C VNA, low frequency (1.0–1.8 GHz) magnetic measurements were carried out on these samples using the broadband Novocontrol Spectrometer.

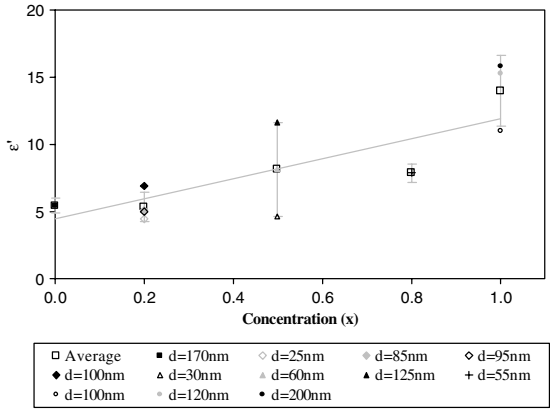


**Figure 1.** Real permittivity of $Co_xNi_{1-x}$ particles at 10 GHz and a volume fraction of 0.25 in paraffin wax.

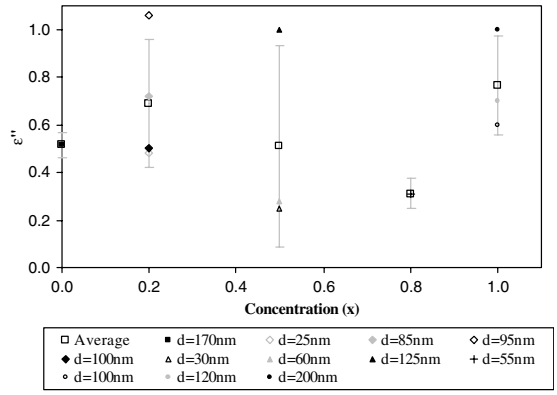


**Figure 2.** Imaginary permittivity of $Co_xNi_{1-x}$ particles at 10 GHz and a volume fraction of 0.25 in paraffin wax.

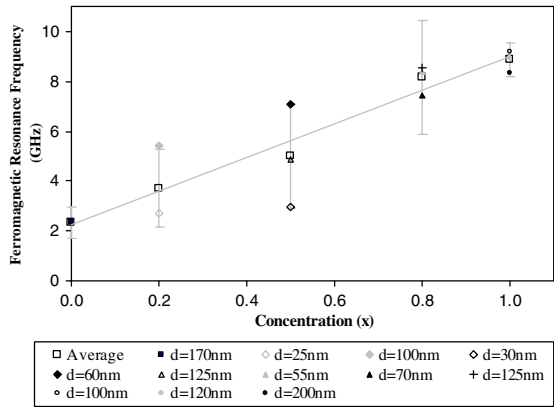


**Figure 3.** Average ferromagnetic resonance frequency positions at different concentrations of $Co_xNi_{1-x}$.

### *3.3. $Co_xNi_{1-x}$ nanoparticle colloid*

A colloid consisting of $Co_{0.8}Ni_{0.2}$ nanoparticles with an average diameter of 100 nm, dispersed in ethylene glycol at 4% by volume, was synthesized within the Energy & Materials Centre at QinetiQ. A sample cell adapted for liquid measurements [1] was used with the HP 8510C VNA to measure the electromagnetic properties of the colloid from 0.5 to 18.0 GHz.

### *3.4. Ferrofluids*

Two ferrofluid samples were purchased from 'Liquids Research Ltd' [4]. The first of the ferrofluids consisted of magnetite particles with an average diameter of 10 nm, dispersed in hydrocarbon oil. The second ferrofluid sample contained cobalt nanoparticles with an average diameter of 5 nm, dispersed in toluene. High frequency measurements (0.5–18.0 GHz) were carried out using the method outlined in the previous section. Low frequency (1.0–1.8 GHz) magnetic measurements were carried out using the broadband Novocontrol Spectrometer.

## 4. Results

### *4.1. $Co_xNi_{1-x}$ nanoparticles*

The permittivity results of $Co_xNi_{1-x}$ dispersions in wax were featureless (as a function of frequency) due to the lack of dielectric resonances and relaxation processes at microwave frequencies. Therefore, spot frequencies are representative of the overall frequency trends. The real and imaginary components of permittivity at 10 GHz were determined for the $Co_xNi_{1-x}$ series at a volume fraction of 0.25. These are shown in figures 1 and 2, along with the average values over the entire size range at each concentration. The error bars relate to the standard deviation of the results. Results across the entire frequency range (0.5–18.0 GHz) are given in [1].

As shown, the overall real permittivity (figure 1) increases linearly with increasing cobalt concentration. However, within each concentration, the results show further variation due to the size of the particles. For example, the results corresponding to $x = 0.2$, 0.5 and 1.0 in figure 1 all show a significant decrease in the real permittivity with decreasing particle size. The trends are consistent with those highlighted by Marquardt *et al* [12], where the decrease in $\varepsilon'$ and $\varepsilon''$ with particle size is attributed to quantum size effects. Size quantization leads to a localization of free carriers, which was shown by Gorkov *et al* [13] to result in reduced ac conductivity and permittivity.

The permeability results obtained for each concentration, particle size and volume fraction were used to determine the ferromagnetic resonance frequency. This was calculated from the maximum value in the imaginary permeability peaks that corresponded to ferromagnetic resonance. The breadth of the ferromagnetic resonance peak was determined from the full width half maximum (FWHM) of the imaginary permeability peak, that is, the full width of the imaginary permeability peak at half its maximum amplitude.

The ferromagnetic resonance frequency corresponding to each particle size, along with the average value over the entire particle size range, is shown in figure 3, with the spread in results calculated using the standard deviation and represented by the error bars.

As shown by figure 3, the ferromagnetic frequency increases with increasing cobalt concentration. The ferromagnetic resonance values are higher than those expected from bulk values using the Kittel equation [14]. However, they are in agreement (after accounting for uncertainties) with those reported by Viau *et al* [15], who showed that the $Co_xNi_{1-x}$ nanoparticle series can produce significantly higher and broader ferromagnetic resonance frequencies than

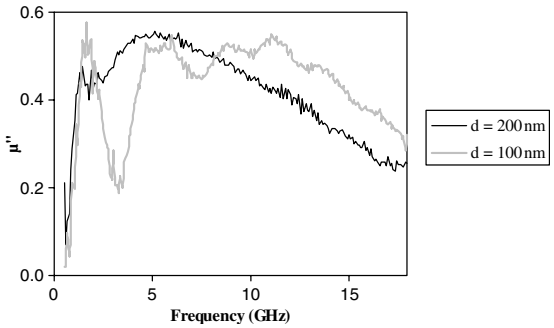


**Figure 4.** Size-related exchange resonance modes in Co particles dispersed in paraffin wax.

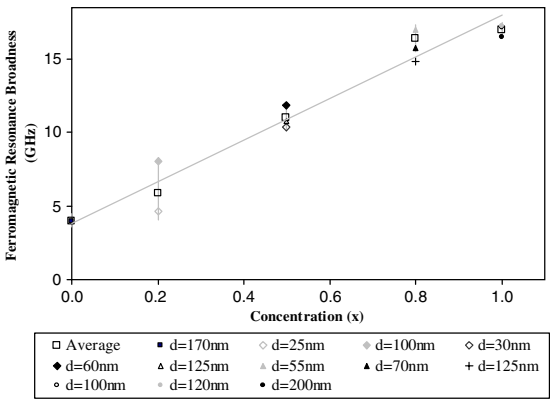


**Figure 5.** Breadth of ferromagnetic resonance peaks at different concentrations of $Co_xNi_{1-x}$.

micron-size particles, due to the presence of the exchange resonance modes [15]. This is apparent from the results corresponding to the individual particle sizes in figure 3.

An example of the exchange resonance modes is given in figure 4, which shows the imaginary permeability of cobalt particles at two different particle sizes. The larger 200 nm diameter cobalt particles exhibit a single resonant peak associated with the magnetostatic mode. However, the 100 nm cobalt particles show a splitting of this peak into additional peaks associated with the exchange resonance modes, which leads to a broadened response. The best comparison with the exchange resonance modes shown in figure 4 is provided by experimental results in [15], where the additional modes are shown to be located at 2, 6, and 12 GHz for 90 nm cobalt particles, which is in agreement with the peak positions shown in figure 4.

Figure 5 shows the frequency breadth (or broadness) of the ferromagnetic resonance peaks at each of the $Co_xNi_{1-x}$ concentrations, $x$. As shown, the breadth of the ferromagnetic resonance peaks can be tuned with relative Co-to-Ni concentration, with breadth increasing linearly with Co concentration, consistent with results in the literature [15].

### 4.2. *Magnetite nanoparticles*

Figures 6 and 7 show the permittivity and permeability responses of the 8 nm diameter magnetite particles.

The results reveal a similar dielectric performance to that of the nickel-rich $Co_xNi_{1-x}$ particles. The permeability results

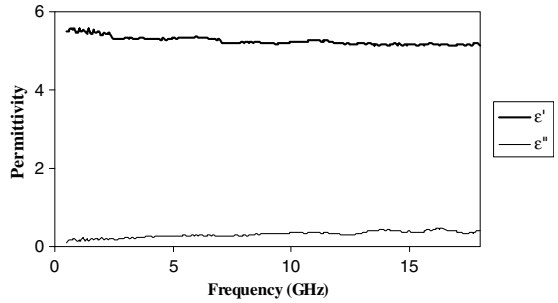


**Figure 6.** Permittivity of 8 nm diameter magnetite ($Fe_3O_4$) particles at a volume fraction of 0.22 in stearic acid.

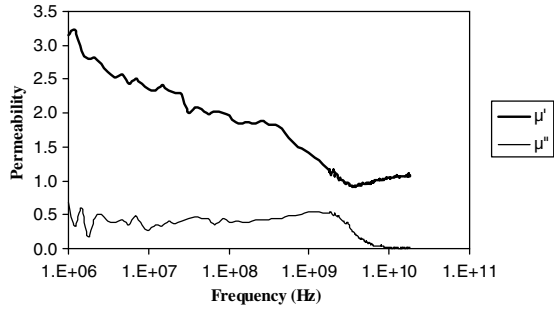


**Figure 7.** Permeability of 8 nm diameter magnetite ($Fe_3O_4$) particles at a volume fraction of 0.22 in stearic acid

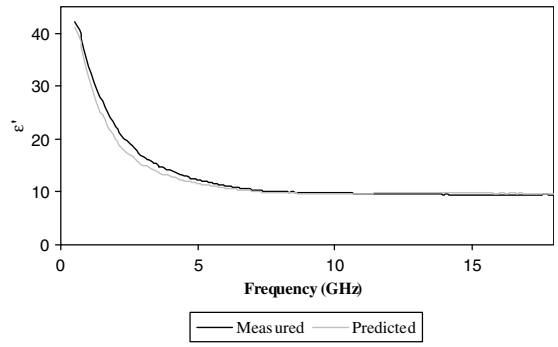


**Figure 8.** Comparison between measured and predicted real permittivity of colloid containing $Co_{0.8}Ni_{0.2}$ particles at 4% by volume in ethylene glycol.

exhibit a relatively low ferromagnetic resonance frequency of 1.5 (±0.2) GHz, which is in agreement with values given in the literature of 1.7 GHz [10]. However, the most significant change in magnetic performance occurs at lower frequencies, where a contribution to the imaginary permeability is produced. This is related to the superparamagnetic loss mechanism, outlined in section 2, which arises due to the single-domain configuration associated with the finite dimensions of the particles, resulting in Néel relaxation.

### 4.3. *$Co_xNi_{1-x}$ nanoparticle colloids*

The performance of a range of $Co_xNi_{1-x}$ colloids was predicted using the results of the $Co_xNi_{1-x}$ dispersions in wax in combination with effective medium theories [5], the latter having been previously validated with the experimental results.

Figures 8–10 present a comparison between measured and predicted results for a colloidal suspension containing

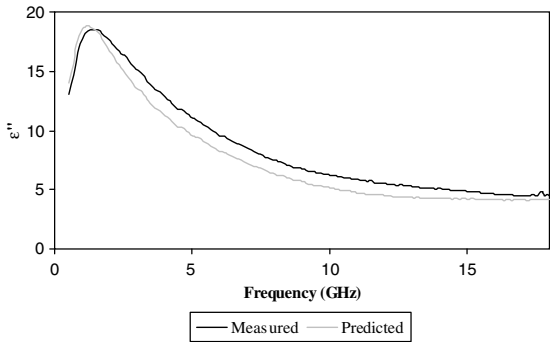


**Figure 9.** Comparison between measured and predicted imaginary permittivity of colloid containing $Co_{0.8}Ni_{0.2}$ particles at 4% by volume in ethylene glycol.

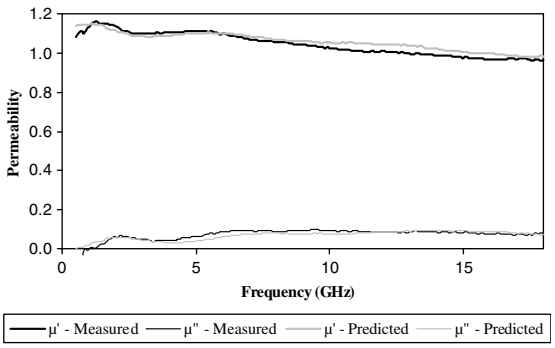


**Figure 10.** Comparison between measured and predicted permeability of colloid containing $Co_{0.8}Ni_{0.2}$ particles at 4% by volume in ethylene glycol.

$Co_{0.8}Ni_{0.2}$ particles, with an average diameter of 100 nm, dispersed in ethylene glycol at 4% by volume. The performance was predicted using the Lichtenecker mixture equation [5], which shows good agreement with the results.

The permeability (figure 10) shows an increment (in comparison with $\mu' = 1$ and $\mu'' = 0$ for non-magnetic materials) attributed to ferromagnetic resonance, with the emergence of some of the characteristics observed from the solid wax dispersions. The position at which this broad resonance is exhibited is consistent with the results discussed in the preceding sections, although the magnitude is reduced due to the low volume fraction. The magnetic data also show the possibility of exchange resonance modes, with the first mode, which was the most prominent in the solid wax dispersions, visible at 2 GHz.

Figures 11 and 12 present the predicted permittivity and permeability, respectively, for a colloid containing $Co_{0.8}Ni_{0.2}$ particles at a volume fraction of 0.15. As shown, a colloid containing such a combination of particles could be used to provide a significant improvement in the electromagnetic properties, resulting from the increase in the permittivity and permeability contributions. A comparison between the imaginary permeability of the measured 4% colloid (figure 10) and the predicted 15% colloid (figure 12) again confirms the possibility of exchange resonance modes emerging in the measured colloid. However, a volume loading of 15% was not achieved experimentally due to problems stabilizing the colloids, related to sedimentation of the particles. Higher volume fractions may be achievable in future colloidal systems

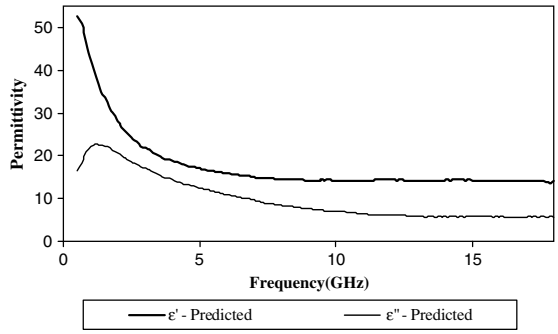


**Figure 11.** Predicted permittivity of colloid containing $Co_{0.8}Ni_{0.2}$ particles at 15% by volume in ethylene glycol.

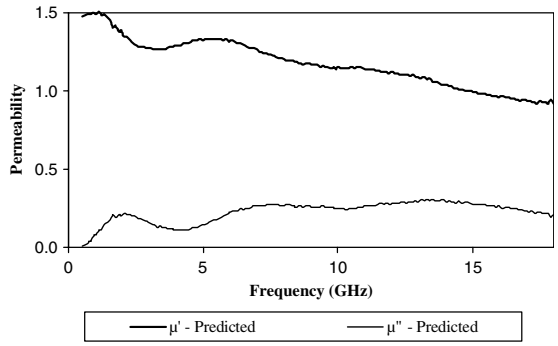


**Figure 12.** Predicted permeability of colloid containing $Co_{0.8}Ni_{0.2}$ particles at 15% by volume in ethylene glycol.

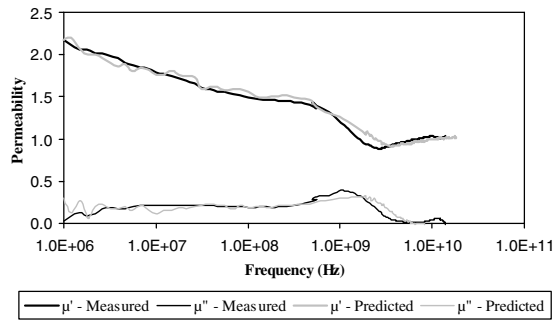


**Figure 13.** Comparison between experimental and predicted permeability of ferrofluid containing 10 nm magnetite particles at 15% by volume.

with smaller particle sizes, which would result in smaller Van der Waals forces between particles and therefore lower sedimentation effects. As shown by figures 11 and 12, such an increase would result in higher levels of dielectric and magnetic loss (i.e. higher imaginary components of permittivity and permeability, respectively) in comparison with the lower volume fraction results demonstrated in figures 8–10.

### *4.4. Ferrofluids*

The purpose of investigating magnetite was to exploit absorption resulting from superparamagnetism, which can be achieved for small particle sizes and low anisotropy constants. Figure 13 presents a comparison between the predicted and measured permeability of a hydrocarbon oil-based ferrofluid, containing magnetite particles with an average particle size of 10 nm and volume fraction of 0.15(±0.05).

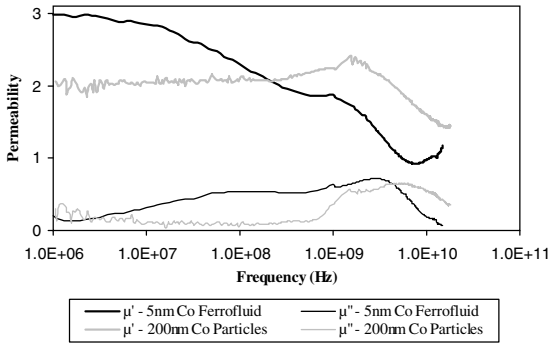


**Figure 14.** Comparison between 200 cm cobalt particles at 30% in wax and ferrofluid containing 5 nm cobalt particles at 15% by volume.

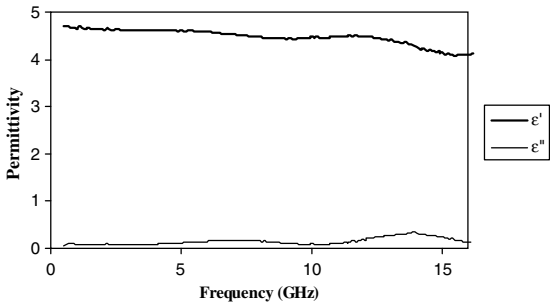


**Figure 15.** Permittivity of ferrofluid containing 5 nm cobalt particles at 15% by volume.

The results show the low frequency Néel relaxation region together with the ferromagnetic resonance peak at higher frequencies, consistent with the solid matrix results demonstrated in figure 7. The ferrofluid performance was predicted using the Lichtenecker mixture equation [5] and the results in figure 7.

Figure 14 shows a comparison between the measured permeability of a toluene-based ferrofluid containing cobalt particles with an average particle size of just 5 nm, at a volume fraction of 0.15($\pm$0.05), and the permeability of 200 nm cobalt particles in paraffin wax, at a volume fraction of 0.30.

The results show a considerable enhancement in the low frequency permeability for the 5 nm cobalt ferrofluid, with the relaxation associated with superparamagnetism providing a contribution to loss. At higher frequencies, loss associated with ferromagnetic resonance is observed for both particle sizes. The Co ferrofluid therefore exhibits broadband magnetic properties ranging from radio to microwave frequencies. This represents a significant improvement over conventional properties, due to the resonant nature of the conventional ferromagnetic loss mechanisms.

Figure 15 shows the corresponding permittivity for the 5 nm cobalt ferrofluid.

The permittivity of the 5nm cobalt ferrofluid shown in figure 15 is significantly lower than the results presented in section 4.1, corresponding to the larger cobalt particle dispersions in wax. The difference in permittivity cannot be entirely accounted for by the differences in the volume fraction. The change in permittivity may therefore again be due to the quantum size effects highlighted in section 4.1. The lower permittivity provides a better impedance match between the material and free space (i.e. lower front-face reflection) as discussed in section 2. Such a colloid could prove beneficial in a range of electromagnetic applications, with potential broadband absorption properties from the radio to the microwave region.

## 5. Conclusions

The results corresponding to $Co_xNi_{1-x}$ nanoparticles show that both the dielectric and the magnetic properties can be controlled through nanoparticle size, as well as through the relative Co-to-Ni concentration. Smaller nanoparticles result in lower permittivities due to quantum size effects, while higher nickel-content particles show lower real components of permittivity in comparison with the higher cobalt concentrations. Nanoparticles in the size range 30–200 nm exhibit broadened ferromagnetic resonance responses, in comparison with conventional micron particle sizes, due to the emergence of exchange resonance modes. Incorporation of these properties into colloidal form has been demonstrated, with the effective medium predictions validated through good agreement with experimental performance. These show that an increase in volume fraction from the experimental value of 0.04 to 0.15 will provide a greater magnetic contribution, better suited to electromagnetic absorption applications.

As particle dimensions decrease to sizes where only single magnetic domains can exist (typically 2–20 nm), an additional magnetic loss mechanism associated with superparamagnetism becomes apparent at radio frequencies, as demonstrated with the Co ferrofluid consisting of 5 nm particles. The superparamagnetic absorption at low frequencies, together with the ferromagnetic resonance at higher frequencies, makes this colloidal combination highly effective with significant broadband loss ranging from radio to microwave frequencies. This makes these colloids the best candidate colloids, amongst those investigated, for enhanced broadband magnetic performance.

## References

[1] Hussain S 2005 The electromagnetic properties of nanoparticle colloids *PhD Thesis* University College London, Ref: 54-13321
[2] Hussain S, Youngs I J and Ford I J 2004 The dielectric properties of charged nanoparticle colloids at radio and microwave frequencies *J. Phys. D: Appl. Phys.* **37** 318
[3] Youngs I J and Bleay S 2002 The interactive age: smart electromagnetic materials *Materials World* **10** (4) 12
[4] Liquids Research Limited, http://www.liquidsresearch.co.uk
[5] Neelakanta P S 1995 *Handbook of Electromagnetic Materials* (London: CRC Press)
[6] Craig D Q M 1995 *Dielectric Analysis of Pharmaceutical Systems* (London: Taylor and Francis)
[7] Pitman K C, Lindley M W, Simkin D and Cooper J F 1991 Radar absorbers: better by design *IEE Proc.* F **138** 223
[8] Bozorth R M 1953 *Ferromagnetism* (London: Macmillan)
[9] Kaiser R and Miskolczy G 1975 Magnetic properties of stable dispersions of subdomain magnetic particles *J. Appl. Phys.* **41** 1064
[10] Fannin P C, Kinsella L and Charles S W 1997 The high frequency complex susceptibility of ferrofluids deduced from fits of lower frequency measurements *J. Phys. D: Appl. Phys.* **30** 533
[11] Novocontrol International, www.novocontrol.com

[12] Marquardt P 1992 Size-governed properties of matrix isolated and percolating mesocopic conductors *J. Electromagn. Waves Appl.* **6** 1197
[13] Gorkov L P and Eliashberg G M 1965 Minute metallic particles in an electromagnetic field *Sov. Phys.—JETP* **21** 940
[14] Kittel C 1948 On the theory of ferromagnetic absorption *Phys. Rev.* **73** 155
[15] Viau G, Fievet-Vincent F, Fievet F, Toneguzzo P, Ravel F and Acher O 1997 Size dependence of microwave permeability of spherical ferromagnetic particles *J. Appl. Phys.* **81** 2749